Environmental Pollution 307 (2022) 119521

Contents lists available at ScienceDirect

Environmental Pollution

journal homepage: www.elsevier.com/locate/envpol

# Responses of reconstituted human bronchial epithelia from normal and health-compromised donors to non-volatile particulate matter emissions from an aircraft turbofan engine☆

Mathilde N. Delaval [a,1,3], Hulda R. Jonsdottir [a,1,9], Zaira Leni [a], Alejandro Keller [b], Benjamin T. Brem [c,4], Frithjof Siegerist [d], David Schönenberger [c,5], Lukas Durdina [c,6], Miriam Elser [c,7], Matthias Salathe [e], Nathalie Baumlin [e], Prem Lobo [f,8], Heinz Burtscher [b], Anthi Liati [g,2], Marianne Geiser [a,*]

[a] Institute of Anatomy, University of Bern, 3012 Bern, Switzerland
[b] Institute for Sensors and Electronics, University of Applied Sciences and Arts Northwestern Switzerland, 5210 Windisch, Switzerland
[c] Empa, Swiss Federal Laboratories for Materials Science and Technology, Laboratory for Advanced Analytical Technologies, 8600 Dübendorf, Switzerland
[d] SR Technics, 8302 Kloten, Switzerland
[e] Department of Internal Medicine, University of Kansas Medical Center, Kansas City, KS, USA
[f] Metrology Research Centre, National Research Council Canada, Ottawa, Ontario K1A 0R6, Canada
[g] Empa, Swiss Federal Laboratories for Materials Science and Technology, Automotive Powertrain Technologies Laboratory, 8600 Dübendorf, Switzerland

ARTICLE INFO

*Keywords:*
Aerosol
Aircraft engine exhaust
Bronchial epithelial cell culture
Cellular response
Non-volatile particulate matter

ABSTRACT

Health effects of particulate matter (PM) from aircraft engines have not been adequately studied since controlled laboratory studies reflecting realistic conditions regarding aerosols, target tissue, particle exposure and deposited particle dose are logistically challenging. Due to the important contributions of aircraft engine emissions to air pollution, we employed a unique experimental setup to deposit exhaust particles directly from an aircraft engine onto reconstituted human bronchial epithelia (HBE) at air-liquid interface under conditions similar to *in vivo* airways to mimic realistic human exposure. The toxicity of non-volatile PM (nvPM) from a CFM56-7B26 aircraft engine was evaluated under realistic engine conditions by sampling and exposing HBE derived from donors of normal and compromised health status to exhaust for 1 h followed by biomarker analysis 24 h post exposure. Particle deposition varied depending on the engine thrust levels with 85% thrust producing the highest nvPM mass and number emissions with estimated surface deposition of $3.17 \times 10^9$ particles $cm^{-2}$ or 337.1 ng $cm^{-2}$. Transient increase in cytotoxicity was observed after exposure to nvPM in epithelia derived from a normal donor as well as a decrease in the secretion of interleukin 6 and monocyte chemotactic protein 1. Non-replicated multiple exposures of epithelia derived from a normal donor to nvPM primarily led to a pro-inflammatory response, while both cytotoxicity and oxidative stress induction remained unaffected. This raises concerns for the long-term implications of aircraft nvPM for human pulmonary health, especially in occupational settings.

☆ This paper has been recommended for acceptance by Admir Créso Targino.

* Corresponding author. Institute of Anatomy, Baltzerstrasse 2, University of Bern, 3012 Bern, Switzerland.
*E-mail address:* marianne.geiser@unibe.ch (M. Geiser).

[1] Equal contribution.
[2] Date of death: April 1, 2021.
[3] Present address: Joint Mass Spectrometry Center (JMSC) at Comprehensive Molecular Analytics (CMA), Helmholtz-Munich, 85764 Neuherberg, Germany.
[4] Present Address: Laboratory of Atmospheric Chemistry, Paul Scherrer Institute, 5232 Villigen, Switzerland.
[5] Present address: Empa, Laboratory for Air Pollution/Environmental Technology, 8600 Dübendorf, Switzerland
[6] Present address: Centre for Aviation, School of Engineering, Zurich University of Applied Sciences, 8401 Winterthur, Switzerland.
[7] Present address: Empa, Automotive Powertrain Technologies Laboratory, 8600 Dübendorf, Switzerland.
[8] Present address: Office of Environment and Energy, Federal Aviation Administration, Washington, D.C. 20591, USA.
[9] Present addresses: 1) Department of Rheumatology, Immunology, and Allergology, Inselspital University Hospital, 3010 Bern, Switzerland. 2) Department of BioMedical Research, University of Bern, 3008 Bern, Switzerland. 3) Spiez Laboratory, Federal Office for Civil Protection, 3700 Spiez, Switzerland.

https://doi.org/10.1016/j.envpol.2022.119521
Received 6 October 2021; Received in revised form 19 May 2022; Accepted 20 May 2022
Available online 24 May 2022

## 1. Introduction

Aircraft engine emissions contribute significantly to both global and local air pollution (Lee et al., 2020). Detailed characterization of these emissions and their adverse health effects is essential for the health and safety of airport workers as well as communities living in proximity of large airports. Due to the continuous growth of commercial air travel, emissions from aircraft engines have contributed to an increase in global air pollution in the last decades and are predicted to keep doing so in the future despite the reduced air-traffic during the COVID-19 pandemic (Manisalidis et al., 2020; Masiol and Harrison, 2014; Mazareanu, 2021; Peeters, 1998; Price and Probert, 1995). Non-volatile particulate matter (nvPM) from aircraft engines is very small, with mean mobility diameters typically smaller than 100 nm, also known as ultrafine particles (UFP), and can traverse the entire human respiratory tract upon inhalation (Lobo et al., 2015; Sturm, 2016a, b). These non-volatile particles are mainly comprised of soot and contain a minor fraction of inorganic, non-combustible ash PM (also referred to as metal-PM). Studies on ash PM, mainly from the automotive sector, have shown that ash consists of metal compounds formed by the combustion of fuel impurities, additives in lubricating oil, as well as metals (*e.g.*, iron, chromium, nickel, copper, tin) from the corrosion and mechanical wear of engine components (Gagné et al., 2021; Liati et al., 2013; Sappok and Wong, 2006; Vaaraslahti et al., 2005). We have previously shown that nvPM from a CFM56-7B26 aircraft engine induces oxidative stress in bronchial epithelial cells at ground-idle (GI) thrust and that the observed biological effects are not determined by deposited particle mass or number alone but rather influenced by particle morphology (Jonsdottir et al., 2019). Furthermore, variability between particle emissions generated by the combustion of fuels with different compositions has been reported, which adds complexity to determining the contribution of aircraft engine emissions to air pollution and its resulting health effects (Jonsdottir et al., 2019; Liati et al., 2019; Saffaripour et al., 2020). Overall, little is known about the general health hazards associated with PM from aircraft engine emissions. However, in recent years, several studies on the composition of aircraft engine exhaust and their effects on pulmonary health have been conducted (Cavallo et al., 2006; Gawron et al., 2020; Habre et al., 2018; He et al., 2020; He et al., 2018; Jonsdottir et al., 2019; Møller et al., 2014; Wing et al., 2020). Thus far, reported results suggest that since PM from aircraft engine emissions shares structural similarities with PM emitted from other combustion sources, particularly diesel exhaust, the resulting health effects would be similar (Bendtsen et al., 2019; He et al., 2020). Furthermore, repeated short (5h) exposures to UFP near a major airport have been associated with decreased lung function in healthy volunteers, further demonstrating the need for comprehensive characterization of aircraft engine emissions and their effects on human health (Lammers et al., 2020). Such studies are especially relevant to airport workers who spend extended periods of time on the tarmac, *e.g.*, baggage handlers, mechanics. Frequent travelers, especially those with underlying respiratory diseases, might also be disproportionally affected.

As previously stated, PM emitted by aircraft engines is small in size, even smaller than that observed in road traffic pollution (Bendtsen et al., 2021; Harris and Maricq, 2001; Stacey, 2019). It is, therefore, able to deposit with high efficiency in the respiratory tract of humans and animals. However, as previously mentioned, absolute quantities of nvPM number and mass from aircraft engines are not the only metrics important to human health. We, and others, have observed a correlation between the physicochemical properties of these combustion-generated particles, both from aircraft and other combustion engines, and adverse health effects (Bendtsen et al., 2020; Jonsdottir et al., 2019). Moreover, the adequate evaluation of the adverse effects of aircraft engines on the human respiratory tract requires the use of a representative model system. In the current study, we exposed reconstituted human bronchial epithelia (HBE) to aircraft engine nvPM at the air-liquid interface, mimicking *in vivo* exposure. These epithelial cell cultures are three-dimensional, pseudostratified, and contain the characteristic epithelial cell types of this lung compartment, such as basal, goblet, and ciliated cells. They produce mucus and exhibit coordinated ciliary beating similar to *in vivo* respiratory epithelium (de Jong et al., 1994; de Jong et al., 1993). In the present study, we evaluated the health effects of nvPM from a CFM56-7B26 aircraft turbofan engine burning standard Jet A-1 fuel at different thrust levels in HBE derived from three individual donors of different background. We deposited nvPM from aircraft engine exhaust directly onto the apical surface of the epithelium under physiological conditions using the portable Nano-Aerosol Chamber for In-Vitro Toxicity (NACIVT) (Jeannet et al., 2015). Additionally, we studied the morphology of the deposited particles by Transmission Electron Microscopy (TEM). The combination of a realistic particle source and a physiological three-dimensional cell culture model provides a unique platform to study the effects of aviation emissions on the human respiratory tract in a controlled experimental set-up.

## 2. Materials & methods

### 2.1. Summary of experimental design

Combustion aerosol was emitted by a CFM56-7B26 turbofan engine and sampled with a standardized sampling system as previously described (Jonsdottir et al., 2019; Liati et al., 2019). To investigate the correlation between nvPM generated at high and low engine thrust levels and cellular effects in pulmonary cells, we sampled aerosols from three distinct thrust levels, 85% (climb-out), 7% (taxi), and ground idle (GI, 3%), along with filtered aerosol (at 65% thrust) as particle-free (P-free) control. The exposure campaign took place in July 2018 at Zürich Airport, Zürich, Switzerland. Aerosol was sampled on 4 consecutive days. We exposed reconstituted primary human bronchial epithelium from three donors of varying background to exhaust at physiological conditions for 1 h. Each individual exposure was repeated two or three times, depending on the availability of cellular material. An overview over number of exposures, replicates, and donors can be found in Table S1. At 24 h post exposure, we assessed distinct biomarkers of pulmonary injury. In addition to physicochemical characterization of the exhaust, we measured the morphology and composition of nvPM by analytical microscopy.

### 2.2. Aerosol generation, sampling, and characterization

An airworthy CFM56-7B26 turbofan engine, running in a test cell at SR Technics at Zürich Airport in Switzerland was used as aerosol source. The engine was fueled with Jet A-1 with fuel properties well within the allowable range for commercial jet fuel. The engine operating conditions were determined using the engine combustor inlet temperature (T3), which correlated to sea-level static thrust levels corrected to international standard atmospheric conditions (15 °C, 1013.25 hPa). This approach has been used for emissions certification of aircraft engines and research experiments (Durdina et al., 2017; ICAO, 2018; Lobo et al., 2020). The aircraft engine nvPM emissions were collected using a single point sampling probe and a standardized sampling system, compliant with the specifications listed in the standards and recommended practices (ICAO, 2017; SAE International, 2018), also used in our previous study (Jonsdottir et al., 2019). Briefly, the extracted nvPM sample is diluted with dry synthetic air by a factor of 8–14 and then transferred to the diagnostic instruments using a 25 m long carbon-loaded, electrically grounded polytetrafluoroethylene line. The nvPM mass concentration was measured using a Micro Soot Sensor (MSS, Model 483, AVL List GmbH, Austria) (Schindler et al., 2004), the nvPM number concentration was determined with an AVL particle counter (APC, Model 489, AVL List GmbH, Austria) (Lobo et al., 2020; Lobo et al., 2015), and particle size distributions were measured with a scanning mobility particle sizer (SMPS, Model 3938, consisting of a long differential mobility analyzer Model 3081A, a soft X-ray aerosol neutralizer Model

3088, and a condensation particle counter Model 3776, TSI Inc., USA). The lower particle size cut-off was 10 nm for the APC (50% of particles counted) and 6 nm for the SMPS measurements. Particle size distribution data from the SMPS were analyzed using Aerosol Instrument Manager (AIM 10.2, TSI Inc.). The SMPS instrument made one scan every 30 s. The reported distributions are averages of multiple scans during the 60-min sampling window. The NACIVT chamber was connected to the diluted PM sampling line in parallel to particle instrumentation. Volatile organic compounds were removed upstream of the NACIVT chamber with a customized low flow thermodenuder (Fierz et al., 2007) operated at 200 °C on the preconditioning and first absorption sections, and 100 °C on the second absorption section. All PM data were plotted using Igor Pro 7.0 (Wavemetrics Inc.) and Origin 2019 (Originlab Inc). Estimated deposition of nvPM onto the apical surface of the reconstituted epithelia was calculated as previously described (Jeannet et al., 2015). General chemical characteristics of Jet-A1 aviation fuel were described previously (Jonsdottir et al., 2019).

### 2.3. Cell cultures

Human bronchial epithelial cells (HBEC) were isolated from human lungs unsuitable for transplantation appropriately consented for donation and recovered by the Life Alliance Organ Recovery Agency (LAORA) Miami (Miami, Florida, USA). The cells were collected from the proximal conducting airways of three individual donors with different background: one normal healthy donor with no smoking history (donor 1) and two asthmatic donors with varying smoking history (donors 2 and 3) (Table S2). Air-Liquid Interface (ALI) cultures of reconstituted HBE were generated as previously described (Jonsdottir and Dijkman, 2015; Künzi et al., 2015; Künzi et al., 2013; Schmid et al., 2010). Briefly, bronchial epithelial cells were maintained in submerged two-dimensional culture in Bronchial Epithelial Cell Growth Medium (BEGM - LHC base media with supplements, Gibco, Fisher Scientific, Reinach, Switzerland). Cells were thereafter seeded onto porous 0.33 $cm^2$ Transwell® inserts (Corning International, Fisher Scientific, Reinach, Switzerland) in chemically defined medium that induces terminal differentiation. Once confluent, apical medium was removed establishing ALI and the epithelium allowed to differentiate over a period of 4 weeks, with apical washes and basal media change three times a week (Jonsdottir and Dijkman, 2015). Terminal differentiation results in a pseudostratified ciliated epithelium with established air-liquid interface. Mucus secretion and ciliary beating were routinely checked visually and by light microscopy, respectively. Differentiated epithelia were washed with Dulbecco's phosphate-buffered saline (DPBS with $Ca^{2+}$ and $Mg^{2+}$, Invitrogen, Lucerne, Switzerland) 1–2 h before aerosol exposure.

### 2.4. Aerosol exposure

Bronchial epithelia derived from three separate human donors were divided into two or three sets of 6 inserts per donor, and each series of inserts was exposed to combustion-generated aerosol from a CFM56-7B26 turbofan engine at different thrust levels (85%, 7% and GI) for 60 min within the NACIVT at physiological conditions, *i.e.*, 37 °C, 5% $CO_2$, and >85% relative humidity on separate days (Table S1). For P-free air exposure, we mounted a Balston DFU Model 9933–11, grade BQ filter (Parker Hannifin Corporation, New York, USA) between the aerosol exhaust line and the thermodenuder. Particle deposition was observed in real-time with Lab View 9.0.1. After exposure, cell cultures were incubated at the same conditions for 1 h before collecting apical wash samples and subsequently incubated for additional 23 h followed by final sampling.

### 2.5. Analyses of cellular responses

To evaluate the cellular effects of the exposure to combustion aerosol, we analyzed several biomarkers at 1 h and/or 24 h post exposure. To assess cytotoxicity, we quantified the release of Adenylate Kinase (AK) by damaged cells into the apical compartment using the commercial ToxiLight kit (LONZA, Visp, Switzerland) according to the manufacturer's instructions. Cytotoxicity is reported as fold AK release over P-free (particle-filtered exhaust) controls. To assess oxidative stress, we analyzed the gene expression of Heme Oxygenase 1 (HMOX-1) by quantitative real-time polymerase chain reaction (qRT-PCR) by extracting total cellular RNA from exposed epithelia with Trizol (Sigma Aldrich, Buchs, Switzerland) and ZymoResearch DirectZol Mini Prep Plus columns (LucernaChem, Luzern, Switzerland) according to the manufacturer's protocol. Complementary DNA (cDNA) was prepared using the QuantiTect® reverse transcription kit (Qiagen, Hombrechtikon, Switzerland) according to the manufacturer's instructions. Briefly, genomic DNA (gDNA) was removed from all samples by incubating extracted RNA in gDNA Wipeout buffer for 2 min at 42 °C and immediately transferring samples to ice. Reverse transcription (RT) of 150 ng total RNA was performed with the provided RT mixes for 15 min at 42 °C and inactivated for 3 min at 95 °C. For gene expression analysis, 0.2 μL of total cDNA was amplified using the Applied Biosystems 7900HT system (Thermo Fisher Scientific) using the following cycling parameters: 15 min at 95 °C, 45 cycles of 15 s at 94 °C, 30 s at 55 °C, and 30 s at 72 °C, followed by a dissociation step to confirm product specificity. Data were normalized to Hypoxanthine-Guanine Phosphoribosyl Transferase (HPRT) using the ΔΔCt method (Livak and Schmittgen, 2001). Biological replicates (n = 3–9 cultures) were analyzed three times using Applied Biosystems SDS v2.4. Data are presented as fold change over P-free controls. The release of the inflammatory mediators, Interleukin (IL)-6, IL-8, and Monocyte Chemoattractant Protein (MCP)-1 into basal media was assessed 24 h after aerosol exposure. Cytokine release was measured using a sandwich Enzyme Linked Immunosorbent Assay (ELISA) according to the manufacturer's instructions (Duoset ELISA; R&D Systems Europe, Abingdon, United Kingdom). All samples were stored at −20 °C from sampling to analysis.

### 2.6. Transmission Electron Microscopy (TEM)

During experiments, nvPM was collected directly on TEM grids, in parallel with cell exposures. Two types of TEM grids were used in the current study: i) Cu-supported holey carbon film grids for detailed study of soot and ii) ultra-thin carbon film grids for better optical contrast facilitating observation of ash particles. TEM imaging was performed with a JEOL 2200FS microscope fitted with an Omega filter, a Schottky field emission gun at 200 kV, and a 0.23 nm point-to-point resolution (Electron Microscopy Center of Empa, Dübendorf, Switzerland). The TEM instrument is equipped with an EDX detector (JEOL EDX detector: EX-24065JGT), which was used for the elemental analysis of the inorganic, ash particles. Gatan DigitalMicrograph® was used for image analysis.

### 2.7. Statistical analysis

Reconstituted epithelia (n = 12–18, *i.e.,* 6 replicates per exposure) were exposed to either aircraft engine exhaust aerosol or to particle-filtered air. The number of biological replicates depended primarily on the availability of cellular material from the different donors and space in the deposition chamber (24 slots). Furthermore, specific focus was put on GI thrust levels based on our previous publication (Jonsdottir et al., 2019), which was analyzed in all donors. Biological data are presented as fold change over P-free control or absolute quantification (pg $mL^{-1}$). Data are presented as mean ± standard deviation (SD). Statistical significance was determined with the commercial software GraphPad Prism 8.0 for Windows (GraphPad Software Inc., La Jolla, California, USA). Non-matching one-way analysis of variance (ANOVA) with Tukey's or Sidak's multiple comparison tests were used for statistical comparison of cytotoxicity and biological responses to negative control (particle-free air exposure). Parameters and applied statistical tests can

be found in the corresponding figure legends. $p$ values $< 0.05$ were considered statistically significant.

## 3. Results

### 3.1. Successful deposition of nvPM from aircraft engine exhaust on reconstituted human bronchial epithelia

Electrometer data collected within the NACIVT deposition chamber show distinct diffusion charging currents for the three thrust levels sampled (Fig. 1a). Currents of $-3995 \pm 340$ fA obtained for 85% thrust indicate the highest particle deposition, while the $-225 \pm 24$ and $-83 \pm 9$ fA registered for GI and 7% thrust, respectively, point to low deposition. Precipitation voltages for P-free exhaust ($-43 \pm 3$ fA) were identical to those observed for synthetic air (SA, dashed line), demonstrating the successful removal of nvPM by the particle filters. The resulting particle size distributions (Fig. 1b) were unimodal and lognormal. Geometric median diameters (GMDs) of particles from GI and 7% thrust are similar at 16.3–16.4 nm. Particles sampled at 85% thrust displayed the largest median diameters at 45.8 nm. Estimated deposition of both mass and number of nvPM from the exhaust onto bronchial epithelia (Fig. 1c and d) was calculated based on Jeannet et al. (2015) and correlates with the observed precipitation voltages from within the chamber, indicating successful deposition of nvPM. The average deposition per surface area of cell culture was $3.17 \times 10^9$ particles $cm^{-2}$ or 337.1 ng $cm^{-2}$ for the 85% thrust condition, $0.22 \times 10^9$ particles $cm^{-2}$ or 0.9 ng $cm^{-2}$ for 7% thrust, and $1.04 \times 10^9$ particles $cm^{-2}$ or 2.3 ng $cm^{-2}$ for GI.

### 3.2. TEM, HRTEM and TEM-EDX analyses of soot and ash collected on TEM grids during exposure

TEM analysis of particles collected at high (85%) and low (GI) thrust level conditions revealed a clear correlation between engine thrust level and the amount of collected soot. It is widely accepted that due to higher surface-to-volume ratio, soot with small particle sizes is more reactive with atmospheric components than that with larger sizes (Al-Qurashi and Boehman, 2008; Harris, 1990; Pahalagedara et al., 2012; Vander Wal et al., 2010; Yehliu et al., 2011). Based on this fact, we determined the size of the soot agglomerates (maximum length) and of their primary particle constituents (diameter of their circular projection, Fig. 2). The results revealed soot agglomerates sampled from 85% thrust conditions are significantly larger (size mode: 60–160 nm, more rarely 200 nm) than those sampled from GI thrust conditions (<40 nm). The size of the primary soot particles within the agglomerates also correlated with thrust levels. The primary soot particles from GI were 5–10 nm, while those from 85% thrust were 10–25 nm, more rarely 30 nm. These results are in line with previous observations (Jonsdottir et al., 2019; Liati et al., 2019; Saffaripour et al., 2020). Ash was present in minor yet detectable amounts among collected particles on examined TEM grids. As characterization of particles by electron microscopy is generally not a quantitative technique, it cannot be implied whether ash can be considered to occur in negligible amounts among nvPM (Gagné et al., 2021). The TEM/EDX analyses of ash under GI conditions revealed that the most

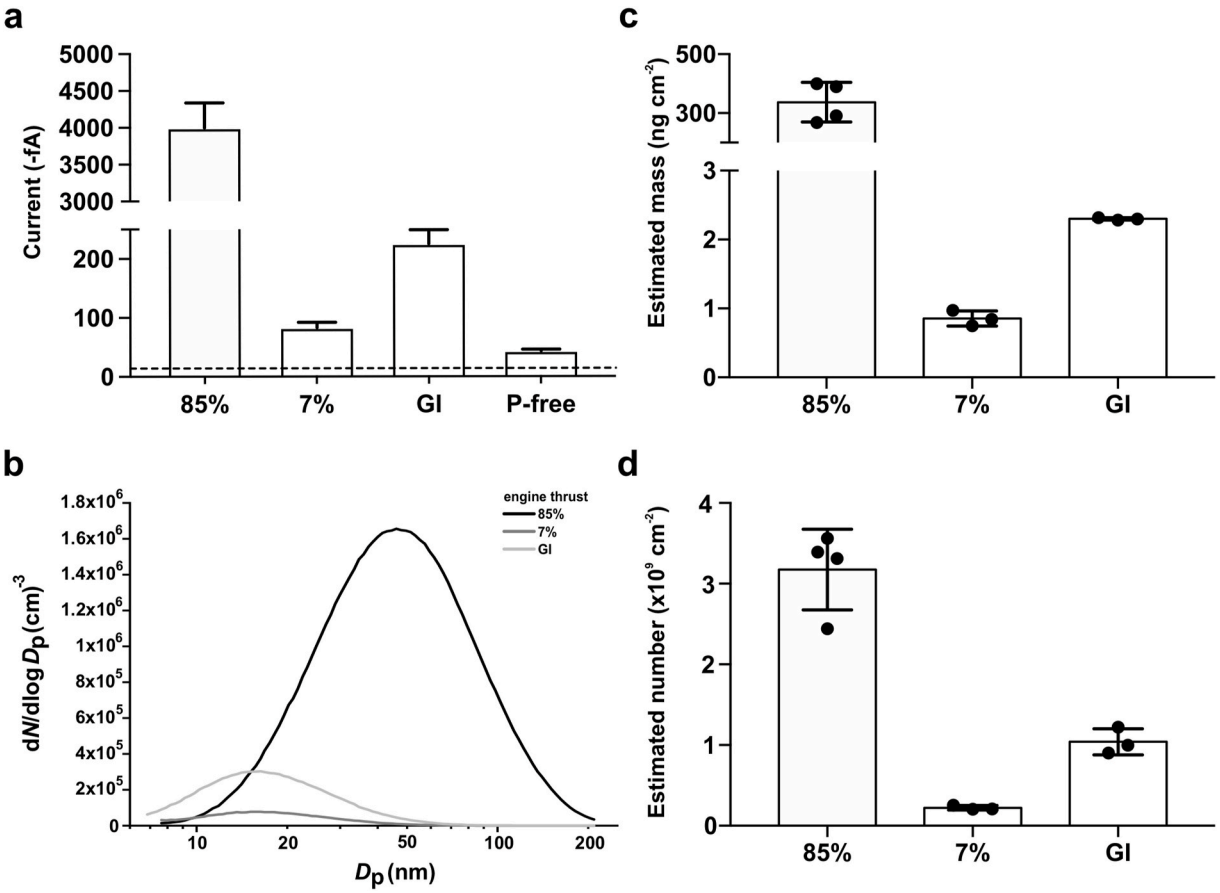


**Fig. 1.** Deposition of non-volatile particulate matter (nvPM) from a CFM56-7B26 turbofan onto reconstituted human bronchial epithelia (HBE). a) Recorded diffusion charging current for each thrust level (0.32mv/fA). **b)** Size distributions of deposited particles. **c)** Mass of nvPM deposited per surface area of cell culture after 1 h of exposure. **d)** Number of nvPM deposited per surface area of cell culture after 1 h of exposure. Highest deposition is observed for 85% thrust and lowest for the second lowest thrust level (7%), which is less deposition than after exposure to ground idle (GI, 3%). Data for diffusion current, particle mass and number are reported as mean and SD of four (85%) or three (7%, GI) independent aerosol generations for cell exposures.

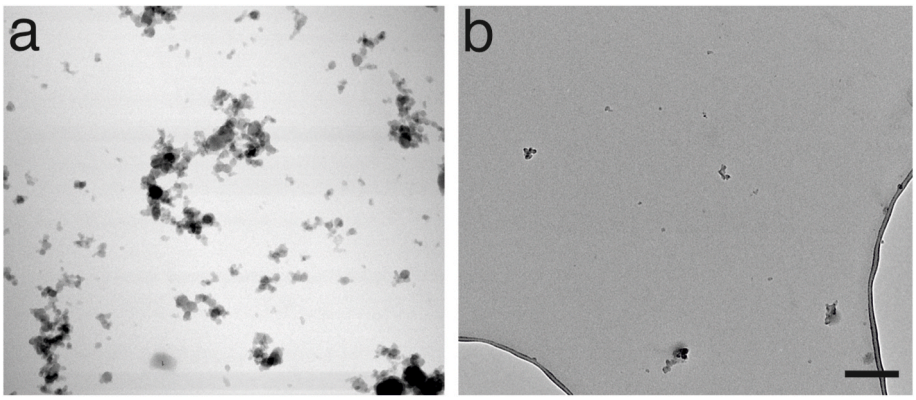


**Fig. 2.** Morphology of non-volatile particulate matter (nvPM) soot emissions. Transmission electron microscopy (TEM) images showing the larger size and higher abundance of soot particles, **a)** at 85% thrust compared to **b)** ground idle (GI) condition. Scale bar: 200 nm.

prominent element is iron (Fe), often together with Chromium (Cr) ± Nickel (Ni) and/or Titanium (Ti), in form of single particles, fragments or aggregates, a few hundreds of nanometers large, rarely down to tens of nanometers. The aggregates themselves consist of tens of nm-large single particles with the same or different chemical composition. Another frequently found element is Calcium (Ca), in the form of an oxide but also together with Sulfur (S) ± Phosphor (P) ± Chloride (Cl). Ca-bearing particles occur as single fragments or as aggregates with sizes of a few hundreds of nanometers. Iron (Fe)- and, more often, Ca-particles were also found inside soot. Other elements detected in ash particles include Aluminum (Al), Magnesium (Mg), Tin (Sn), Silicon (Si), and more rarely Potassium (K), Manganese (Mn), Zinc (Zn) and Bismuth (Bi), the latter a few tens of nanometers large. Analysis of ash from high engine thrust conditions (85%) revealed the same chemical composition as that from low (GI) thrust. However, Silver (Ag) was identified repeatedly in high thrust ash samples with sizes of a few tens of nm. Ash particle sizes, in general, were similar among both examined thrust conditions.

### *3.3. Biological responses in epithelia from a normal donor after 1 h of exposure to nvPM*

Exposures to both GI and 7% thrust led to a statistically significant, immediate (1 h), two-fold increase of AK release in normal cells (donor 1) compared to control cells exposed to P-free air ($p < 0.0001$ and $p = 0.0001$, respectively) (see Fig. 3). This increase of AK release is also observed at 24 h post exposure to 7% thrust, although at lower level ($p = 0.0144$). There was no significant increase in cytotoxicity over P-free controls after exposure to nvPM at 85% thrust. There was no correlation between deposited particle mass or number and the observed cytotoxicity. Exposure to nvPM from 7% thrust led to a statistically significant decrease in the release of both the pro-inflammatory cytokine IL-6 ($p = 0.0092$) and the chemokines MCP-1 ($p = 0.253$) and IL-8 ($p = 0.0299$) compared to P-free controls. MCP-1 levels also decreased after exposure to GI thrust ($p = 0.0024$).

### *3.4. Comparison of biological responses after 1 h of exposure to ground idle thrust in epithelia from three individual donors*

Comparison of the same biological parameters in epithelia derived from three separate donors and exposed to GI thrust revealed significant differences in the release of adenylate kinase (AK) at 1 h and 24 h post exposure (Fig. 4a) and the secretion of MCP-1 at 24-h post exposure (Fig. 4c) for donor 1. The epithelia from the two additional donors did not exhibit any alterations in the tested parameters at 24 h post exposure. Additionally, the overall biological responses of epithelia derived from donors 2 and 3 were similar apart from baseline secretions of IL-8, which were higher in epithelia of donor 3 (Fig. 4c).

### *3.5. Non-replicated analysis of biological responses after multiple exposures to nvPM emissions in a normal donor*

To determine the adverse effects of multiple exposures to nvPM from distinct thrust levels, we exposed normal HBE (donor 1) to high (85%) and low (7%) engine thrust levels for 1 h, once a day for up to 3 days (Figure S1). Multiple exposures to nvPM at 7% thrust did not lead to an increase in cytotoxicity, while a single exposure caused a significant, immediate increase of AK release (average 1.6-fold, $p < 0.05$) that had resolved 24 h post exposure. Furthermore, nvPM from 7% thrust induced a significant, non-dose dependent decrease of IL-6 ($p < 0.01$–$p < 0.05$) and a significant, dose-dependent decrease of MCP-1 ($p < 0.001$–$p < 0.0001$), similar to 85% thrust. However, multiple exposures to 7% thrust did not affect IL-8 levels, unlike 85% thrust, which caused an almost two-fold increase of IL-8 after the second exposure ($p < 0.0001$) compared to controls. A second exposure to 85% thrust induced a decrease of MCP-1 ($p < 0.001$) compared to P-free controls. Multiple exposures to nvPM of low and high engine thrust levels did not induce significant changes in the expression of the HMOX-1 gene, indicating low oxidative stress.

## 4. Discussion

In the present study, we evaluated the respiratory health effects of nvPM from a CFM56-7B26 turbofan, one of the most commonly used aircraft engines in the world, by using a unique experimental setup for particle sampling and cellular deposition. We sampled nvPM directly from the engine exhaust under representative operating conditions and deposited the particles onto the apical surface of reconstituted bronchial epithelia (HBE) to evaluate their effects on acute toxicity and inflammation. This unique combination of experimental systems is able to realistically represent *in vivo* particle deposition in the human airways. Furthermore, we assessed these effects in HBE from single donors of normal and compromised health status, providing a relevant overview of the potential adverse respiratory effects of nvPM from aircraft engine exhaust.

The nvPM emission profiles of the CFM56-7B26 turbofan engine have been extensively characterized in previous studies (Brem et al., 2015; Durdina et al., 2021; Lobo et al., 2020). The nvPM mass-based emissions have been found to be higher at engine levels corresponding to idle (3–7% thrust), decreasing to a minimum at 15–30% engine thrust levels, and then increasing to maximum rated thrust. Similarly, the nvPM number-based emissions are higher at engine idle and decrease a low engine thrust levels, however, they increase up to 60% thrust and then decrease again to maximum rated thrust. The size distributions vary with engine thrust levels, with geometric mean diameter of particles ranging from ca. 10 nm–40 nm (Durdina et al., 2021; Lobo et al., 2020). Furthermore, the particle effective density has been observed to

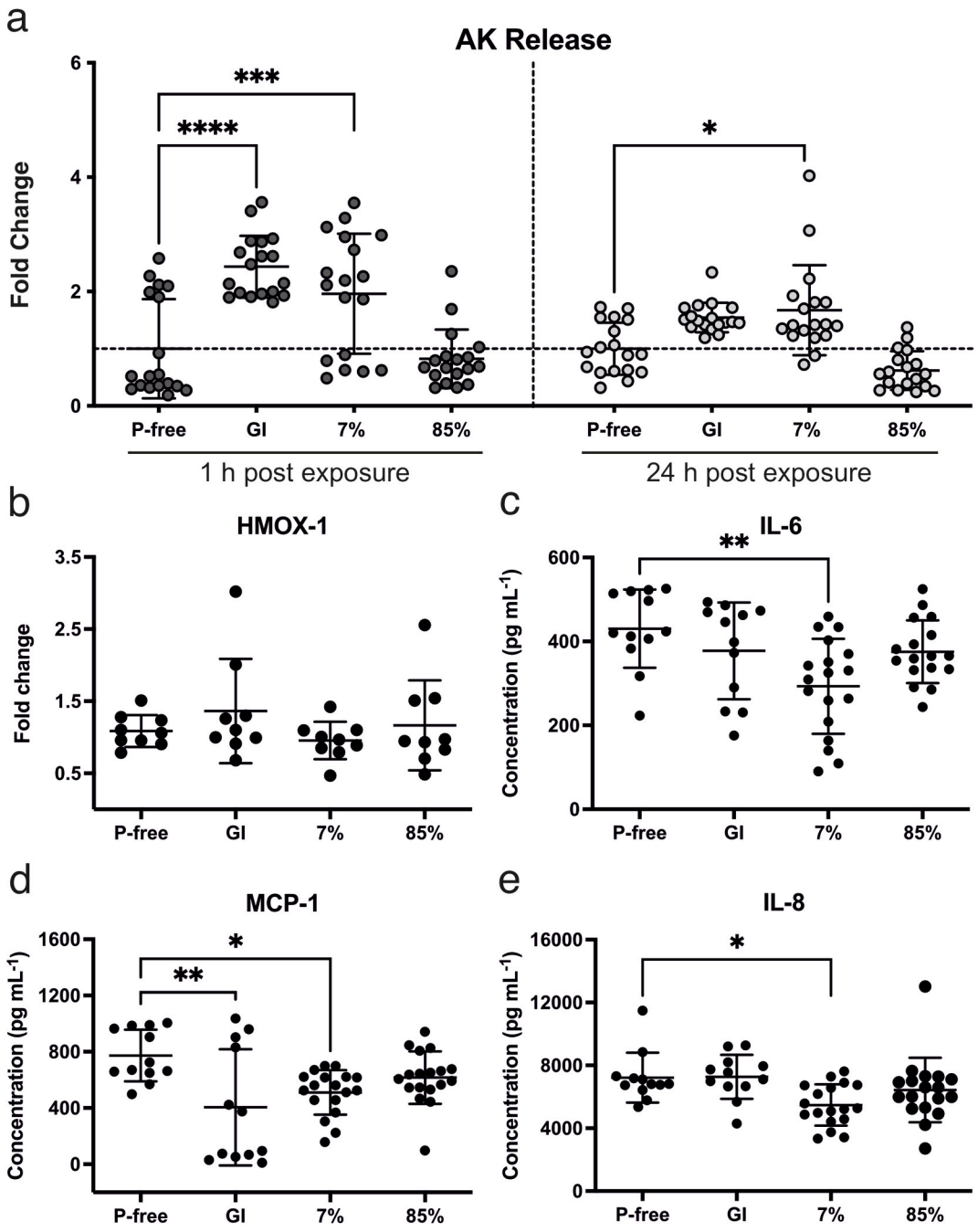


**Fig. 3.** Biological responses in bronchial epithelia of a normal donor after 1 h of exposure to non-volatile particulate matter (nvPM) from different thrust levels. a) Adenylate kinase (AK) released from damaged cells into the apical compartment, presented as fold change over particle-filtered (P-free) controls, at 1 h and 24 h post exposure (hpe). **b)** HMOX-1 gene expression 24 hpe as determined by qPCR, presented as fold change over P-free controls. **c)** IL-6, **d)** MCP-1, and **e)** IL-8 secretions into the basal compartment 24 hpe as determined by ELISA, presented as pg $mL^{-1}$. Data is presented as mean ± SD and n = 9–18 cultures from three independent exposures. Statistical significance was assessed using a non-matching two-way analysis of variance (ANOVA) with Sidak's multiple comparison test (AK release) or a non-matching one-way analysis of variance (ANOVA) with Tukey's multiple comparison test (HMOX-1, IL-6, MCP-1, IL-8): $^{*}p < 0.05$, $^{**}p < 0.01$, $^{***}p < 0.001$, and $^{****}p < 0.0001$.

increase with engine thrust levels and decrease with particle size (Abegglen et al., 2015; Durdina et al., 2014). The chemical composition and radiative properties of nvPM emissions from the CFM56-7B26 have also been reported (Elser et al., 2019).

Upon exposure to nvPM from three distinct engine thrust levels, we observed immediate damage in epithelia derived from a normal donor (donor 1), especially after exposure to lower thrust levels (7% and GI), indicating that this observed effect is not related to either nvPM mass or number, since the highest nvPM deposition was observed after exposure to 85% thrust. This is in line with other published studies as well as our previous observations (BéruBé et al., 2007; Jaramillo et al., 2018; Jonsdottir et al., 2019; Schmid and Stoeger, 2016). Exposure to PM emissions is known to interfere with inflammatory cytokine homeostasis, where both up- and down-regulation of modulators have been reported in both experimental and human studies (Bendtsen et al., 2019; Habre et al., 2018; He et al., 2020; He et al., 2018). However, most current studies on the biological effects of aircraft emissions cover total PM and do not focus on non-volatile PM specifically. For instance, mice

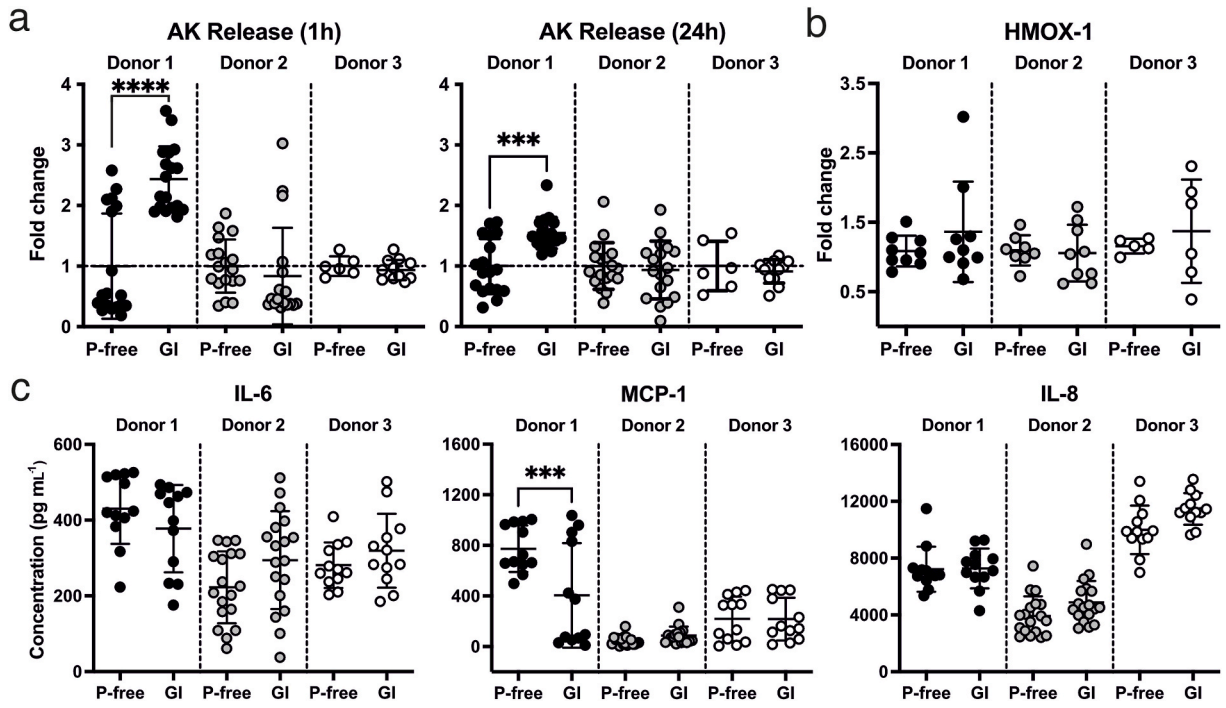


**Fig. 4.** Comparison of biological responses after 1 h of exposure to ground idle thrust conditions in three individual donors. a) Adenylate kinase (AK) released from damaged cells into the apical compartment, presented as fold change over particle-free (P-free) controls, at 1 and 24 h post exposure (hpe). **b)** HMOX-1 gene expression 24 hpe as determined by qPCR, presented as fold change over P-free controls. **c)** IL-6, MCP-1, and IL-8 secretions into the basal compartment 24 hpe as determined by ELISA, presented as pg $mL^{-1}$. Data is presented as mean ± SD and $n = 9$–18 cultures from three independent exposures. Statistical significance was assessed using a non-matching one-way analysis of variance (ANOVA) with Tukey's multiple comparison test (HMOX-1, IL-6, MCP-1, IL-8): ***$p < 0.001$, and ****$p < 0.0001$.

exposed to total PM from aircraft exhaust for up to 90 days displayed an acute inflammation with immune cell influx to the lungs, which persisted for up to 28 days (Bendtsen et al., 2019). Additionally, Habre et al. detected acute systemic inflammation, characterized by increased circulation of the pro-inflammatory cytokine IL-6 in asthmatic, non-smoking adults exposed to total UFP downwind of Los Angeles International Airport (LAX) for 2 h (Habre et al., 2018). In the present study, we did not observe an increase in IL-6 release in any donor after single 1-h exposures. Increased expression of IL-6 has also been observed in bronchial epithelial cell lines exposed to both low and high doses of UFP from aircraft exhaust (He et al., 2020; He et al., 2018) and those results are in line with our previous observations with the undifferentiated human bronchial cell line, BEAS-2B (Jonsdottir et al., 2019). In contrast, here we observed a decrease in the secretion of IL-6, MCP-1, and IL-8 in epithelia from a normal donor after exposure to 7% thrust. Secretion of MCP-1 also decreased after exposure to GI thrust. Non-repeated analysis of multiple exposures of the normal donor to nvPM appeared to down-regulate the inflammatory response even further. No significant changes in cytokine secretions were observed in the other two donors.

We previously observed an increase in acute cellular toxicity and oxidative stress in BEAS-2B cells after exposure to ground idle (GI) thrust using the same experimental setup (Jonsdottir et al., 2019). Similarly, in the present study, exposure to GI and 7% thrust conditions resulted in increased cytotoxicity in epithelia derived from a normal donor (donor 1) 1 h post exposure. After 24 h, only epithelia exposed to 7% thrust exhibit minor increased cytotoxicity. In contrast to our previous study with BEAS-2B cells, we found no increase in the expression of HMOX-1 in any donor after exposure to any thrust condition, indicating that re-differentiated human bronchial cells are more robust, when it comes to the induction of the oxidative stress response compared to two-dimensional BEAS-2B cells. Additionally, this could indicate that 1-h exposures are simply not long enough to induce drastic changes in reconstituted airway epithelia. The airways are in constant contact with various types of aerosols throughout our lives and having a high tolerance for aerosol exposures would be pertinent to their function. Furthermore, we did not observe any effect of GI aerosol exposure in HBE cultures of the health-compromised donors (donors 2 and 3). We consider it very likely that, in general, diseased epithelia are more susceptible to damage from nvPM exposure and therefore, we hypothesize that this could be related to the asthmatic background and smoking history of these donors, since their derived bronchial epithelia show characteristics of diseased epithelium. In the present study, we combined a state-of-the art sampling system coupled to a realistic aerosol source with complex three-dimensional cell cultures and conducted aerosol exposures at physiological conditions. This experimental system is unique but not without its limitations. While this study was conducted with more physiologically relevant cell culture models, we could only analyze one donor per health status. Although this limits the generality of our results, we still consider these data a strong basis for further investigation into the likely adverse health effects from exposure to aircraft exhaust. Additionally, although the reconstituted epithelia used here is comprised of many different cell types, we are only able to elucidate the epithelial response to aerosol exposure due to the absence of an immune system or cells of the adjoining connective tissue (*i.e.*, fibroblasts, endothelial cells). However, given that the respiratory epithelium is the entry point of emission aerosols, the epithelial response is likely to represent a sizable portion of the resulting effects making it a strongly relevant experimental parameter. Though exposure times were realistic, they were also limited due to the operational schedule of the engine test cell and fuel costs. Longer exposures may have potentially resulted in an increased epithelial response.

Despite these limitations, we attempted to cover a broad variety of parameters and found that adverse effects do not seem to be primarily related to deposited nvPM mass and number, since very low doses of nvPM (7%, GI) did cause significant cytotoxicity in normal HBE. The size

of nvPM (below 100 nm) is inversely proportional to its surface reactivity, which could explain the higher effect of nvPM from the two lowest thrust levels, in comparison to those from 85% thrust. Generally, physicochemical characterization of the particles is necessary to fully understand the potential adverse effects caused by nvPM. Here, we observed a clear correlation between engine thrust levels and the number, as well as the size of soot agglomerates and their primary particle constituents. GI thrust produced substantially fewer and smaller soot particles than those from 85% thrust, correlating with electrometer data obtained from within the deposition chamber. Based on the difference in size of the soot particles collected under different engine thrust levels, soot from GI thrust is more reactive than that collected from 85% thrust, which may explain the toxicological effects observed in response to nvPM from low engine thrust levels. There was no difference in ash particle size observed among the different thrust level conditions. Compared to soot, ash production occurs in minute amounts and the most frequent element in ash is iron (Fe), either alone or in combination with Chromium (Cr), Nickel (Ni), and/or Titanium (Ti), mainly derived from corrosion and the mechanical wear of engine components. Other observed metallic components from combustion of fuel and/or lube oil additives were primarily Ca ± S ± P ± Cl, less frequently Al, Mg, Sn, Si, more rarely K, Mn, Zn, Bi, and, at high thrust levels, Ag. Based on these physicochemical properties, aircraft exhaust particles are similar to those in diesel exhaust (Bendtsen et al., 2021).

Realistic *in vitro* exposures are crucial to comprehensively decipher the effects of UFP on human health and this includes using representative doses for human exposure. In this study, we exposed pulmonary epithelia to realistic doses of nvPM from three separate thrust levels, *i.e.*, climb-out (85%), taxi (7%) and ground idle (3%). Here, the deposited mass of particles ranged from 0.9 ng $cm^{-2}$ to 337.1 ng $cm^{-2}$ after 1 h of exposure, covering the range of ambient exposures to high daily occupational exposures (Paur et al., 2011). Although airport workers are mainly exposed to particles generated at low thrust levels, particles emitted at high levels are also relevant to human exposure and health, since the air mass in and around the airport is constantly being mixed and influenced by both airport schedules and prevailing winds. Indeed, Buonanno et al. found that particle number concentrations measured in the vicinity of the runway present several main short-term peaks during the workday, related to take-off and landing of aircraft and pre-flight operations. They measured an average total concentration of $6.5 \times 10^3$ particles $cm^{-3}$ at a static receptor site. However, when measuring the occupational exposure to airborne particles and other pollutants at the airport, it could be as high as $2.5 \times 10^4$ particles $cm^{-3}$ and these exposure levels vary depending on the role of the worker at the airport (Buonanno et al., 2012). Similarly, Møller et al. found that baggage handlers are exposed to more ultrafine particles than employees working inside the airport. Levels of exposure were evaluated from $5 \times 10^3$ UFP $cm^{-3}$ for inside workers up to $3.7 \times 10^4$ UFP $cm^{-3}$ for baggage handlers (Møller et al., 2014). However, these studies seem to report particle number concentrations on the lower end (Masiol and Harrison, 2014). Furthermore, the study of a cohort of male workers at the Copenhagen airport may shed much needed light on the incidence of respiratory diseases developed and/or exacerbated in relation to aircraft exhaust exposure by estimating the contribution of aviation related UFP to total personal exposure (Møller et al., 2017). In this context, our study highlights the importance of evaluating the effects of aircraft exhaust nvPM, even at a low dose, since surface exposure as low as $1 \times 10^9$ particles $cm^{-2}$ and 1 ng $cm^{-2}$ can cause a biological response, especially in health-compromised epithelia.

## 5. Conclusions

Toxicological data on the adverse health effects of particles emitted by aircraft engines are still scarce. This is partly due to general experimental difficulty, *i.e.*, particle collection at the airport and performing realistic *in vitro* and *in vivo* toxicity studies relevant to the human health hazard and risk assessments. Here, using a unique experimental setup for particle sampling directly from the engine running under representative thrust conditions and an instrument specifically developed to mimic inhalation exposure, we demonstrated that exposure to non-volatile particle matter causes biological responses in epithelia derived from three single donors of different background. Our results support the need to further characterize the pulmonary toxicity of aircraft engine exhaust and reinforce the need for establishing Occupational Exposure Limits (OELs) for such particles to protect airport workers, especially those with underlying respiratory conditions. Based on the current data, clarifications of the adverse effects of multiple exposures to nvPM from aircraft emissions should be of specific interest to both airport employees and neighboring communities.

## Funding sources

This research was supported by the Swiss Federal Office for Civil Aviation (FOCA), Bern Switzerland, projects 2016–037 (granted to M. G.) and 2015–113 (granted to B.T.B.). M.S. and N.B. acknowledge funding by the National Heart, Lung and Blood Institute (NHLBI), United States, grants R01 HL133240 and R01 HL157942.

## Data availability

All relevant raw data are available from the authors upon reasonable request.

## CRediT authorship contribution statement

**Mathilde N. Delaval:** Investigation, Data curation, Formal analysis, Methodology, Validation, Visualization, Writing – original draft, Writing – review & editing. **Hulda R. Jonsdottir:** Conceptualization, Investigation, Data curation, Formal analysis, Methodology, Supervision, Validation, Visualization, Writing – original draft, Writing – review & editing. **Zaira Leni:** Methodology, Writing – review & editing. **Alejandro Keller:** Data curation, Formal analysis, Methodology, Validation, Visualization, Writing – review & editing. **Benjamin T. Brem:** Data curation, Methodology, Validation, Funding acquisition, Writing – review & editing. **Frithjof Siegerist:** Resources. **David Schönenberger:** Resources, Methodology. **Lukas Durdina:** Investigation, Data curation, Formal analysis, Methodology, Visualization, Writing – review & editing. **Miriam Elser:** Investigation, Data curation, Formal analysis, Methodology, Writing – review & editing. **Matthias Salathe:** Methodology, Validation, Writing – review & editing. **Nathalie Baumlin:** Methodology, Validation. **Prem Lobo:** Investigation, Data curation, Formal analysis, Methodology, Writing – review & editing. **Heinz Burtscher:** Investigation, Methodology, Writing – review & editing. **Anthi Liati:** Formal analysis, Data curation, Methodology, Validation, Visualization, Writing – original draft. **Marianne Geiser:** Conceptualization, Data curation, Funding acquisition, Methodology, Project administration, Supervision, Validation, Writing – original draft, Writing – review & editing.

## Declaration of competing interest

The authors declare that they have no known competing financial interests or personal relationships that could have appeared to influence the work reported in this paper.

## Acknowledgements

We thank Y. Arroyo, Electron Microscopy Center, Empa, for assistance during TEM imaging.

## Appendix A. Supplementary data

Supplementary data to this article can be found online at https://doi.org/10.1016/j.envpol.2022.119521.

## References


Abegglen, M., Durdina, L., Brem, B.T., Wang, J., Rindlisbacher, T., Corbin, J.C., Lohmann, U., Sierau, B., 2015. Effective density and mass–mobility exponents of particulate matter in aircraft turbine exhaust: dependence on engine thrust and particle size. J. Aerosol Sci. 88, 135–147.

Al-Qurashi, K., Boehman, A.L., 2008. Impact of exhaust gas recirculation (EGR) on the oxidative reactivity of diesel engine soot. Combust. Flame 155, 675–695.

Bendtsen, K.M., Bengtsen, E., Saber, A.T., Vogel, U., 2021. A review of health effects associated with exposure to jet engine emissions in and around airports. Environ. Health 20, 10.

Bendtsen, K.M., Brostrøm, A., Koivisto, A.J., Koponen, I., Berthing, T., Bertram, N., Kling, K.I., Dal Maso, M., Kangasniemi, O., Poikkimäki, M., Loeschner, K., Clausen, P.A., Wolff, H., Jensen, K.A., Saber, A.T., Vogel, U., 2019. Airport emission particles: exposure characterization and toxicity following intratracheal instillation in mice. Part. Fibre Toxicol. 16, 23.

Bendtsen, K.M., Gren, L., Malmborg, V.B., Shukla, P.C., Tunér, M., Essig, Y.J., Krais, A. M., Clausen, P.A., Berthing, T., Loeschner, K., Jacobsen, N.R., Wolff, H., Pagels, J., Vogel, U.B., 2020. Particle characterization and toxicity in C57BL/6 mice following instillation of five different diesel exhaust particles designed to differ in physicochemical properties. Part. Fibre Toxicol. 17, 38.

Brem, B.T., Durdina, L., Siegerist, F., Beyerle, P., Bruderer, K., Rindlisbacher, T., Rocci-Denis, S., Andac, M.G., Zelina, J., Penanhoat, O., Wang, J., 2015. Effects of fuel aromatic content on nonvolatile particulate emissions of an in-production aircraft gas turbine. Environ. Sci. Technol. 49, 13149–13157.

Buonanno, G., Bernabei, M., Avino, P., Stabile, L., 2012. Occupational exposure to airborne particles and other pollutants in an aviation base. Environ. Pollut. 170, 78–87.

BéruBé, K., Balharry, D., Sexton, K., Koshy, L., Jones, T., 2007. Combustion-derived nanoparticles: mechanisms of pulmonary toxicity. Clin. Exp. Pharmacol. Physiol. 34, 1044–1050.

Cavallo, D., Ursini, C.L., Carelli, G., Iavicoli, I., Ciervo, A., Perniconi, B., Rondinone, B., Gismondi, M., Iavicoli, S., 2006. Occupational exposure in airport personnel: characterization and evaluation of genotoxic and oxidative effects. Toxicology 223, 26–35.

de Jong, P.M., van Sterkenburg, M.A., Hesseling, S.C., Kempenaar, J.A., Mulder, A.A., Mommaas, A.M., Dijkman, J.H., Ponec, M., 1994. Ciliogenesis in human bronchial epithelial cells cultured at the air-liquid interface. Am. J. Respir. Cell Mol. Biol. 10, 271–277.

de Jong, P.M., van Sterkenburg, M.A., Kempenaar, J.A., Dijkman, J.H., Ponec, M., 1993. Serial culturing of human bronchial epithelial cells derived from biopsies. In Vitro Cell. Dev. Biol. Anim. 29a, 379–387.

Durdina, L., Brem, B.T., Abegglen, M., Lobo, P., Rindlisbacher, T., Thomson, K.A., Smallwood, G.J., Hagen, D.E., Sierau, B., Wang, J., 2014. Determination of PM mass emissions from an aircraft turbine engine using particle effective density. Atmos. Environ. 99, 500–507.

Durdina, L., Brem, B.T., Elser, M., Schönenberger, D., Siegerist, F., Anet, J.G., 2021. Reduction of nonvolatile particulate matter emissions of a commercial turbofan engine at the ground level from the use of a sustainable aviation fuel blend. Environ. Sci. Technol. 55, 14576–14585.

Durdina, L., Brem, B.T., Setyan, A., Siegerist, F., Rindlisbacher, T., Wang, J., 2017. Assessment of particle pollution from jetliners: from smoke visibility to nanoparticle counting. Environ. Sci. Technol. 51, 3534–3541.

Elser, M., Brem, B.T., Durdina, L., Schönenberger, D., Siegerist, F., Fischer, A., Wang, J., 2019. Chemical composition and radiative properties of nascent particulate matter emitted by an aircraft turbofan burning conventional and alternative fuels. Atmos. Chem. Phys. 19, 6809–6820.

Fierz, M., Vernooij, M.G.C., Burtscher, H., 2007. An improved low-flow thermodenuder. J. Aerosol Sci. 38, 1163–1168.

Gagné, S., Couillard, M., Gajdosechova, Z., Momenimovahed, A., Smallwood, G., Mester, Z., Thomson, K., Lobo, P., Corbin, J.C., 2021. Ash-decorated and ash-painted soot from residual and distillate-fuel combustion in four marine engines and one aviation engine. Environ. Sci. Technol. 55, 6584–6593.

Gawron, B., Białecki, T., Janicka, A., Zawiślak, M., Górniak, A., 2020. Exhaust toxicity evaluation in a gas turbine engine fueled by aviation fuel containing synthesized hydrocarbons. Aircraft Eng. Aero. Technol. 92, 60–66.

Habre, R., Zhou, H., Eckel, S.P., Enebish, T., Fruin, S., Bastain, T., Rappaport, E., Gilliland, F., 2018. Short-term effects of airport-associated ultrafine particle exposure on lung function and inflammation in adults with asthma. Environ. Int. 118, 48–59.

Harris, S., Maricq, M.M., 2001. Signature size distributions for diesel and gasoline engine exhaust particulate matter. J. Aerosol Sci. 32, 749–764.

Harris, S.J., 1990. Surface growth and soot particle reactivity. Combust. Sci. Technol. 72, 67–77.

He, R.-W., Gerlofs-Nijland, M.E., Boere, J., Fokkens, P., Leseman, D., Janssen, N.A.H., Cassee, F.R., 2020. Comparative toxicity of ultrafine particles around a major airport in human bronchial epithelial (Calu-3) cell model at the air–liquid interface. Toxicol. Vitro 68, 104950.

He, R.-W., Shirmohammadi, F., Gerlofs-Nijland, M.E., Sioutas, C., Cassee, F.R., 2018. Pro-inflammatory responses to PM0.25 from airport and urban traffic emissions. Sci. Total Environ. 640–641, 997–1003.

ICAO, 2017. Environmental Protection: Vol. II Aircraft Engine Emissions. In: Annex 16 to the Convention on International Civil Aviation, fourth ed. ICAO, Montréal.

ICAO, 2018. Environmental Protection: Vol. II Aircraft Engine Emissions. In: Annex 16 to the Convention on International Civil Aviation, fourth ed. ICAO, Montréal.

Jaramillo, I.C., Sturrock, A., Ghiassi, H., Woller, D.J., Deering-Rice, C.E., Lighty, J.S., Paine, R., Reilly, C., Kelly, K.E., 2018. Effects of fuel components and combustion particle physicochemical properties on toxicological responses of lung cells. J. Environ. Sci. Health, Part A 53, 295–309.

Jeannet, N., Fierz, M., Kalberer, M., Burtscher, H., Geiser, M., 2015. Nano aerosol chamber for in-vitro toxicity (NACIVT) studies. Nanotoxicology 9, 34–42.

Jonsdottir, H.R., Delaval, M., Leni, Z., Keller, A., Brem, B.T., Siegerist, F., Schönenberger, D., Durdina, L., Elser, M., Burtscher, H., Liati, A., Geiser, M., 2019. Non-volatile particle emissions from aircraft turbine engines at ground-idle induce oxidative stress in bronchial cells. Communications Biology 2, 90.

Jonsdottir, H.R., Dijkman, R., 2015. Characterization of human coronaviruses on well-differentiated human airway epithelial cell cultures. Methods Mol. Biol. 1282, 73–87.

Künzi, L., Krapf, M., Daher, N., Dommen, J., Jeannet, N., Schneider, S., Platt, S., Slowik, J.G., Baumlin, N., Salathe, M., Prévôt, A.S.H., Kalberer, M., Strähl, C., Dümbgen, L., Sioutas, C., Baltensperger, U., Geiser, M., 2015. Toxicity of aged gasoline exhaust particles to normal and diseased airway epithelia. Sci. Rep. 5, 11801.

Künzi, L., Mertes, P., Schneider, S., Jeannet, N., Menzi, C., Dommen, J., Baltensperger, U., Prévôt, A.S.H., Salathe, M., Kalberer, M., Geiser, M., 2013. Responses of lung cells to realistic exposure of primary and aged carbonaceous aerosols. Atmos. Environ. 68, 143–150.

Lammers, A., Janssen, N.A.H., Boere, A.J.F., Berger, M., Longo, C., Vijverberg, S.J.H., Neerincx, A.H., Maitland - van der Zee, A.H., Cassee, F.R., 2020. Effects of short-term exposures to ultrafine particles near an airport in healthy subjects. Environ. Int. 141, 105779.

Lee, D.S., Fahey, D.W., Skowron, A., Allen, M.R., Burkhardt, U., Chen, Q., Doherty, S.J., Freeman, S., Forster, P.M., Fuglestvedt, J., Gettelman, A., De León, R.R., Lim, L.L., Lund, M.T., Millar, R.J., Owen, B., Penner, J.E., Pitari, G., Prather, M.J., Sausen, R., Wilcox, L.J., 2020. The Contribution of Global Aviation to Anthropogenic Climate Forcing for 2000 to 2018. Atmospheric Environment, p. 117834.

Liati, A., Schreiber, D., Alpert, P.A., Liao, Y., Brem, B.T., Corral Arroyo, P., Hu, J., Jonsdottir, H.R., Ammann, M., Dimopoulos Eggenschwiler, P., 2019. Aircraft soot from conventional fuels and biofuels during ground idle and climb-out conditions: electron microscopy and X-ray micro-spectroscopy. Environ. Pollut. 247, 658–667.

Liati, A., Schreiber, D., Dimopoulos Eggenschwiler, P., Arroyo Rojas Dasilva, Y., 2013. Metal particle emissions in the exhaust stream of diesel engines: an electron microscope study. Environ. Sci. Technol. 47, 14495–14501.

Livak, K.J., Schmittgen, T.D., 2001. Analysis of relative gene expression data using real-time quantitative PCR and the 2(-Delta Delta C(T)) Method. Methods 25, 402–408.

Lobo, P., Durdina, L., Brem, B.T., Crayford, A.P., Johnson, M.P., Smallwood, G.J., Siegerist, F., Williams, P.I., Black, E.A., Llamedo, A., Thomson, K.A., Trueblood, M. B., Yu, Z., Hagen, D.E., Whitefield, P.D., Miake-Lye, R.C., Rindlisbacher, T., 2020. Comparison of standardized sampling and measurement reference systems for aircraft engine non-volatile particulate matter emissions. J. Aerosol Sci. 145, 105557.

Lobo, P., Durdina, L., Smallwood, G.J., Rindlisbacher, T., Siegerist, F., Black, E.A., Yu, Z., Mensah, A.A., Hagen, D.E., Miake-Lye, R.C., Thomson, K.A., Brem, B.T., Corbin, J.C., Abegglen, M., Sierau, B., Whitefield, P.D., Wang, J., 2015. Measurement of aircraft engine non-volatile PM emissions: results of the aviation-particle regulatory instrumentation demonstration experiment (A-PRIDE) 4 campaign. Aerosol. Sci. Technol. 49, 472–484.

Manisalidis, I., Stavropoulou, E., Stavropoulos, A., Bezirtzoglou, E., 2020. Environmental and health impacts of air pollution: a review. Front. Public Health 8.

Masiol, M., Harrison, R.M., 2014. Aircraft engine exhaust emissions and other airport-related contributions to ambient air pollution: a review. Atmos. Environ. 95, 409–455.

Mazareanu, E., 2021. Air Traffic - Passenger Growth Rates Forecast 2019-2040. https://www.statista.com/statistics/269919/growth-rates-for-passenger-and-cargo-air-traffic/.

Møller, K.L., Brauer, C., Mikkelsen, S., Loft, S., Simonsen, E.B., Koblauch, H., Bern, S.H., Alkjær, T., Hertel, O., Becker, T., Larsen, K.H., Bonde, J.P., Thygesen, L.C., 2017. Copenhagen Airport Cohort: air pollution, manual baggage handling and health. BMJ Open 7, e012651.

Møller, K.L., Thygesen, L.C., Schipperijn, J., Loft, S., Bonde, J.P., Mikkelsen, S., Brauer, C., 2014. Occupational exposure to ultrafine particles among airport employees - combining personal monitoring and global positioning system. PLoS One 9, e106671.

Pahalagedara, L., Sharma, H., Kuo, C.-H., Dharmarathna, S., Joshi, A., Suib, S.L., Mhadeshwar, A.B., 2012. Structure and oxidation activity correlations for carbon blacks and diesel soot. Energy Fuels 26, 6757–6764.

Paur, H.-R., Cassee, F.R., Teeguarden, J., Fissan, H., Diabate, S., Aufderheide, M., Kreyling, W.G., Hänninen, O., Kasper, G., Riediker, M., Rothen-Rutishauser, B., Schmid, O., 2011. In-vitro cell exposure studies for the assessment of nanoparticle toxicity in the lung—a dialog between aerosol science and biology. J. Aerosol Sci. 42, 668–692.

Peeters, J.H.A.M., 1998. Aviation and air pollution. In: Schneider, T. (Ed.), Studies in Environmental Science. Elsevier, pp. 601–613.

Price, T., Probert, D., 1995. Environmental impacts of air traffic. Appl. Energy 50, 133–162.
SAE International, 2018. ARP 6320 Procedure for the Continuous Sampling and Measurement of Non-volatile Particulate Matter Emissions from Aircraft Turbine Engines. SAE International, Warrendale.
Saffaripour, M., Thomson, K.A., Smallwood, G.J., Lobo, P., 2020. A review on the morphological properties of non-volatile particulate matter emissions from aircraft turbine engines. J. Aerosol Sci. 139, 105467.
Sappok, A.G., Wong, V.W., 2006. Comparative Particulate Trap Performance Using Fischer-Tropsch and Conventional Diesel Fuels in a Modern CI Engine, ASME 2006 Internal Combustion Engine Division Spring Technical Conference, pp. 93–107.
Schindler, W., Haisch, C., Beck, H.A., Niessner, R., Jacob, E., Rothe, D., 2004. A photoacoustic sensor system for time resolved quantification of diesel soot emissions. SAE International.
Schmid, A., Sutto, Z., Schmid, N., Novak, L., Ivonnet, P., Horvath, G., Conner, G., Fregien, N., Salathe, M., 2010. Decreased soluble adenylyl cyclase activity in cystic fibrosis is related to defective apical bicarbonate exchange and affects ciliary beat frequency regulation. J. Biol. Chem. 285, 29998–30007.
Schmid, O., Stoeger, T., 2016. Surface area is the biologically most effective dose metric for acute nanoparticle toxicity in the lung. J. Aerosol Sci. 99, 133–143.
Stacey, B., 2019. Measurement of ultrafine particles at airports: a review. Atmos. Environ. 198, 463–477.
Sturm, R., 2016a. Local lung deposition of ultrafine particles in healthy adults: experimental results and theoretical predictions. Ann. Transl. Med. 4, 420-420.
Sturm, R., 2016b. Total deposition of ultrafine particles in the lungs of healthy men and women: experimental and theoretical results. Ann. Transl. Med. 4, 234-234.
Vaaraslahti, K., Keskinen, J., Giechaskiel, B., Solla, A., Murtonen, T., Vesala, H., 2005. Effect of lubricant on the formation of heavy-duty diesel exhaust nanoparticles. Environ. Sci. Technol. 39, 8497–8504.
Vander Wal, R.L., Bryg, V.M., Hays, M.D., 2010. Fingerprinting soot (towards source identification): physical structure and chemical composition. J. Aerosol Sci. 41, 108–117.
Wing, S.E., Larson, T.V., Hudda, N., Boonyarattaphan, S., Fruin, S., Ritz, B., 2020. Preterm birth among infants exposed to in utero ultrafine particles from aircraft emissions. Environ. Health Perspect. 128, 047002.
Yehliu, K., Vander Wal, R.L., Boehman, A.L., 2011. A comparison of soot nanostructure obtained using two high resolution transmission electron microscopy image analysis algorithms. Carbon 49, 4256–4268.